

## Unstable displacement defects and hydrogen trapping in GaAs

H. J. Stein and J. C. Barbour

*Sandia National Laboratories, Albuquerque, New Mexico 87185-1056*

(Received 24 March 1997)

Defects produced by implantation of hydrogen into GaAs at 80 K have been investigated. Upon implantation, a predominant absorption band at  $2029\text{ cm}^{-1}$  for As-H centers is observed. A  $10\text{-cm}^{-1}$  full width at half maximum at 80 K for the band, and strong dependence of the frequency and bandwidth on measurement temperature, are indicative of bonding of hydrogen at displacement defects within the lattice. Results from annealing show loss of As-H centers between 180 and 250 K with an activation energy of  $0.5\pm 0.5\text{ eV}$ . Characteristics for As-H center annealing are compared to those reported previously for atomic displacement disorder in irradiated GaAs. Release of hydrogen from As-H bonds within thermally unstable damage regions is suggested to explain the annealing loss of As-H centers. An increase in absorption by Ga-H centers upon loss of As-H centers is attributed to retrapping of hydrogen on Ga neighbors of  $V_{\text{As}}$  or on  $V_{\text{As}}\text{-As}_i$  pair defects. [S0163-1829(97)03231-1]

### I. INTRODUCTION

Hydrogen can interact with defects in bulk material and at interfaces to passivate electronic states,<sup>1</sup> and can introduce vibrational states for hydrogen in the resulting centers.<sup>1-3</sup> Such hydrogen interactions are utilized for defect decoration in fundamental defect studies,<sup>1-3</sup> and for passivation of defects in device structures.<sup>4</sup> Infrared (IR) absorption is a primary investigative tool for the detection of localized vibrational modes (LVM's) that result from the bonding of hydrogen at defects in semiconductor and dielectric materials.<sup>1-3</sup> Dependence of a LVM frequency on the hydrogen isotope can establish assignment of modes to hydrogen, and dependence on the atomic constituents of the host lattice facilitates assignment of the bonding site for hydrogen within the lattice.

Unlike Si, where electron paramagnetic resonance (EPR) provided definitive identification for many defects,<sup>5</sup> EPR has been less useful for defect identification in III-V compound semiconductors. More reliance, therefore, is placed upon IR absorption and other experimental techniques for defect characterization and identification in III-V compounds.<sup>1,3</sup> Implantation of GaAs with hydrogen at room temperature produces a LVM for Ga-H bonds detected by IR absorption.<sup>1,6-8</sup> It is widely accepted that these bonds form at As vacancy ( $V_{\text{As}}$ ) or Frenkel pair ( $V_{\text{As}}\text{-As}_i$ ) displacement defects on the As sublattice.<sup>1,6-8</sup> It is known from irradiation damage studies on GaAs, however, that significant defect annealing can occur below room temperature<sup>9-12</sup> so that the Ga-H centers may not be the initial bonding site for hydrogen. Relatively little use has been made of hydrogen interactions for decoration and characterization of defects that are unstable below room temperature in compound semiconductors.

Described herein are results from an IR absorption study on the formation and annealing of hydrogen-decorated defects in GaAs created by hydrogen ion implantation at 80 K. Surprisingly, the initial bonding of hydrogen implanted into GaAs at 80 K is found to occur primarily with As rather than Ga. The resultant As-H centers, however, are unstable and

removed by annealing below room temperature. We have measured the kinetics and energetics for annealing of the As-H centers, and the characteristics for the As-H centers are compared to those for defect reordering below room temperature in radiation-damaged GaAs.

### II. EXPERIMENTAL DETAILS

A high resistivity 3-in.-diam  $\langle 100 \rangle$  Czochralski GaAs wafer was polished on both sides to a thickness of  $635\text{ }\mu\text{m}$  and diced into  $0.63\times 0.63\text{-cm}$  samples for the studies of defect formation and trapping of hydrogen implanted into GaAs. Samples were clamped with an interlayer indium foil to a copper cold finger of a liquid nitrogen refrigerant cryostat.<sup>13</sup> Implantations were performed at energies between 100 and 330 keV at 80 K. A gate valve and optical windows on a rotatable body of the cryostat allowed removal of the cryostat from the ion implanter and insertion into the sample chamber of a Nicolet 60SX Fourier transform infrared (FTIR) spectrometer. The sample was maintained at the implantation temperature during transfer of the cryostat from the implanter to the FTIR spectrometer. Spectra were acquired to have  $4\text{-cm}^{-1}$  resolution. Isochronal and isothermal annealing was performed within the cryostat. A resistance heater and heat exchanger positioned between the sample and a liquid nitrogen reservoir in the cryostat is capable of producing a rapid increase in the sample temperature ( $\approx 50\text{ K/min}$ ) for temperatures between 80 and 200 K. The rapid increase occurs after an initial delay required to boil liquid from the heat exchanger. Temperature at a set point was controlled to  $\pm 1\text{ K}$  with a Beckman 7200 series digital controller, which sensed the output from a chromel-constantan thermocouple fastened to the cold finger near the sample.

### III. EXPERIMENTAL RESULTS

Absorption bands at  $1834$  and  $2029\text{ cm}^{-1}$  produced by hydrogen-ion implantation of GaAs at 80 K are shown in Fig. 1. Spectra are plotted for successive implantations of ions at 330, 300, 250, 200, and 150 keV into both optical

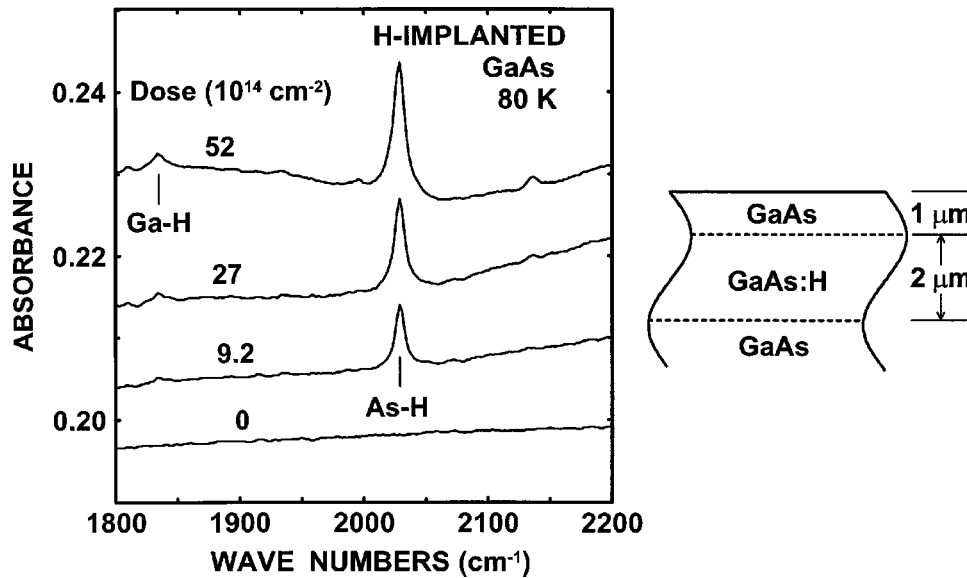


FIG. 1. Absorption bands at 2029 and 1834  $\text{cm}^{-1}$  for As-H and Ga-H centers in GaAs after hydrogen implantations and measurements at 80 K. Spectra are arbitrarily displaced on the absorbance axis for presentation.

faces of the sample. Doses at the different energies were scaled to produce a nearly uniform concentration of hydrogen in a  $\approx 2\text{-}\mu\text{m}$ -thick layer buried  $1\ \mu\text{m}$  below the surface, according to the TRIM-90 calculation program.<sup>14</sup> For the doses per face listed in Fig. 1, the corresponding average hydrogen concentrations in the buried layers are approximately  $4.6 \times 10^{18}$ ,  $1.4 \times 10^{19}$ , and  $2.6 \times 10^{19}\ \text{cm}^{-3}$ . The spectra show an increase of intensities for absorption bands at 1834 and 2029  $\text{cm}^{-1}$  with an increase in hydrogen dose. Thus, the results are consistent with assignment of these two bands to stretch vibrational modes for hydrogen bonded to the host constituents. While additional weak bands appear in the spectra and increase with ion dose, the emphasis in the present work is on the formation and annealing of the two major bands.

Plotted in Fig. 2 are spectra showing the effects of 20-min isochronal annealing on the 2029- and 1834- $\text{cm}^{-1}$  bands for temperatures between 80 and 300 K. Hydrogen had been introduced into the GaAs by implantations at energies of 250, 200, 150, and 100 keV to a total dose of  $2.5 \times 10^{15}\ \text{cm}^{-2}$  into each of the two optical faces. The resultant hydrogen concentrations is  $\approx 1.7 \times 10^{19}\ \text{cm}^{-3}$  in  $1.5\text{-}\mu\text{m}$  thick layers buried about  $0.7\ \mu\text{m}$  below the surface. The spectra in Fig. 2 show that the intensity of the 2029- $\text{cm}^{-1}$  band remains nearly constant through 150 K, but decreases strongly in the 200-K annealing step. In contrast, the intensity for the 1834- $\text{cm}^{-1}$  band *increases* slowly upon annealing at 200, 250, and 300 K.

The 1834- $\text{cm}^{-1}$  band has been observed previously<sup>2,6-8</sup> following hydrogen implantation at room temperature, and it has been assigned to a stretch vibrational mode for Ga—H bonds.<sup>2,6-8</sup> The 2029  $\text{cm}^{-1}$  in hydrogen-implanted GaAs has been assigned to a stretch mode for As—H bonds.<sup>15</sup> Assignments for the Ga-H and As-H bands are firmly based upon frequency shifts produced by hydrogen isotope substitution, upon substitution of the group III and group V constituents (e.g., InAs and InP substituted for the GaAs host<sup>15</sup>), and upon correspondence of the observed frequencies to those for Ga—H and As—H bonds in solids. We will subsequently,

therefore, refer to the 1834- and 2029- $\text{cm}^{-1}$  bands as bands for Ga-H and As-H centers, respectively.

Preferential formation of As-H centers under hydrogen implantation is apparent in the spectra of Fig. 2. In contrast, the formation of Ga-H centers occurs predominantly during subsequent annealing when hydrogen that is released from As-H centers is available for retrapping. The maximum intensity for the Ga-H absorption band is only one-half that for the initial As-H band. It is not known if this difference is caused by a lower oscillator strength for Ga—H than for As—H bonds, or if it is an indication of the hydrogen re trapping efficiency.

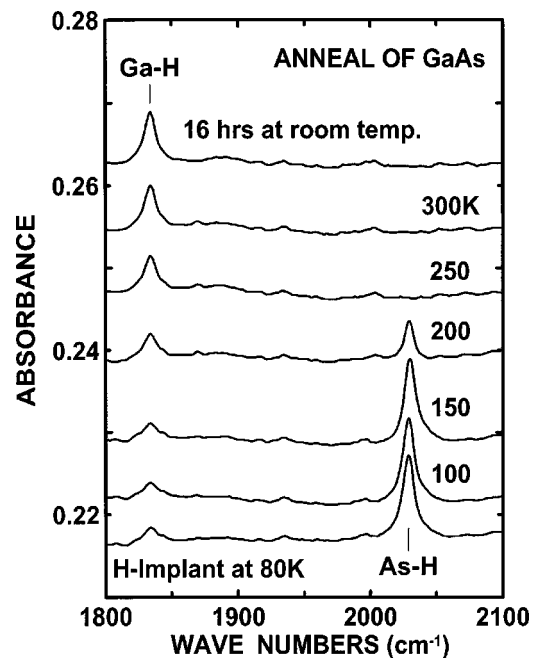


FIG. 2. Isochronal annealing data between 80 and 300 K for As-H and Ga-H centers after implantation of  $2.5 \times 10^{15}\text{-cm}^{-2}$  hydrogen ions into each of two optical faces. Spectra are arbitrarily displaced on absorbance axis for presentation.

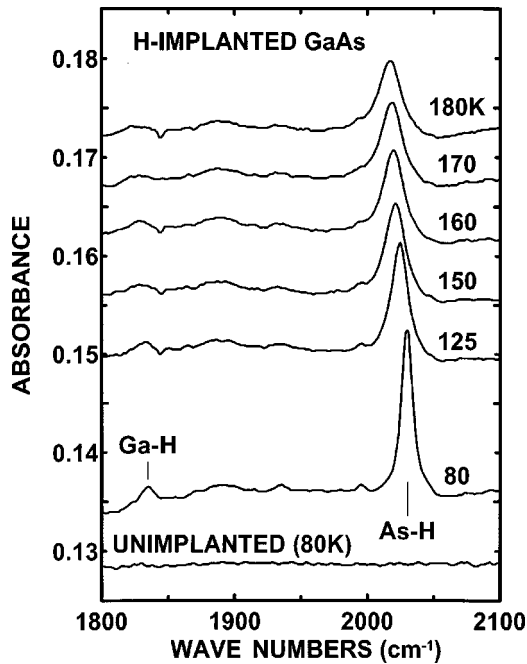


FIG. 3. Effect of measurement temperature on the As-H absorption bandwidth and frequency. Spectra are arbitrarily displaced on the absorbance axis for presentation.

The As-H band frequency and bandwidth as a function of the measurement temperature between 80 and 180 K are shown in Fig. 3. The measurements were made after sequential implantations of hydrogen ions at 330, 300, 250, 200, 150, and 100 keV at 80 K to a dose of  $10^{15} \text{ cm}^{-2}$  for each energy into both optical faces. The maximum temperature for the measurements was limited by an onset of annealing of the As-H band. An annealing step was performed at 170 K before the measurements to stabilize the displacement damage in the sample to this temperature. The band frequency and bandwidth at half maximum taken from the data of Fig. 3 are plotted in Fig. 4 where the dashed line represents a decrease of  $0.13 \text{ cm}^{-1}/\text{deg}$  for the frequency. There is a com-

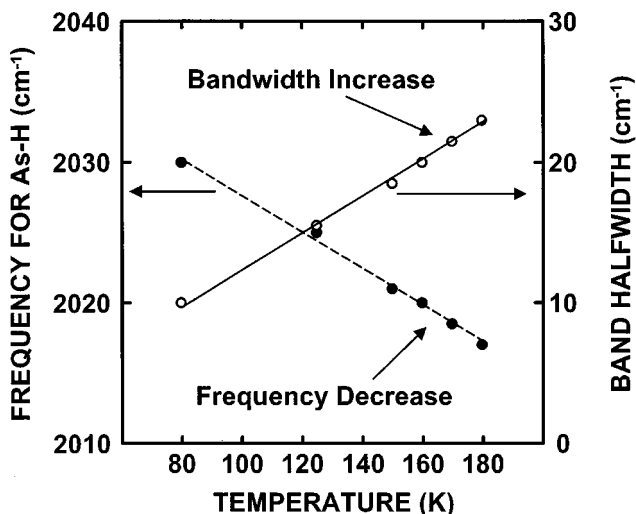


FIG. 4. Center frequency and bandwidth versus measurement temperature for As-H absorption band in hydrogen-implanted GaAs.

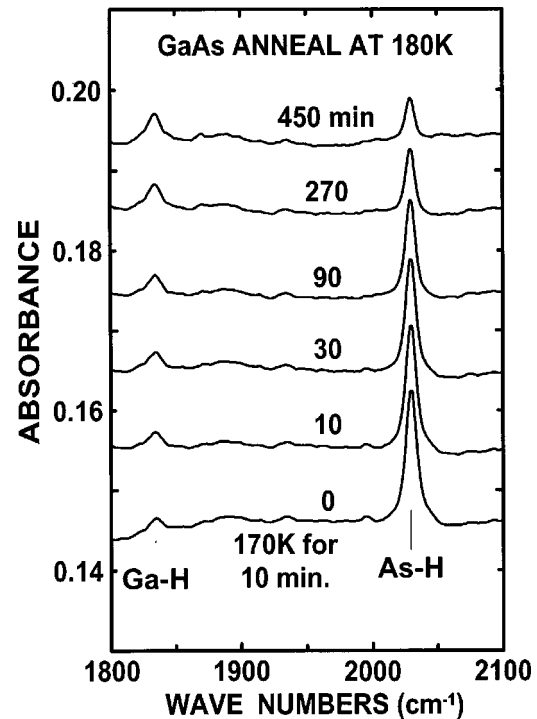


FIG. 5. Isothermal annealing data at 180 K for As-H and Ga-H centers after implantation of  $6 \times 10^{15} \text{ cm}^{-2}$  hydrogen ions into each of two optical faces. Spectra are arbitrarily displaced on the absorbance axis for presentation.

parable rate of increase in the bandwidth with temperature as shown by the solid line. The changes in frequency and bandwidth with temperature for the As-H band are in the direction of, but larger in magnitude than, those for thermal effects in an undamaged lattice.<sup>1</sup>

The same doses and ion energies listed in the previous paragraph were used to produce a set of samples for isothermal annealing experiments. The samples were annealed for 10 min at 170 K before beginning isothermal annealing at 180, 190, and 200 K. Isothermal annealing of the As-H band at 180 K is shown in the spectra of Fig. 5. These spectra indicate a continued loss of the As-H band intensity, and an increase in Ga-H band intensity for 450 min of annealing at 180 K. Similar isothermal annealing data were also acquired at 190 and 200 K.

Unannealed fractions for the As-H centers determined from the peak intensities for the  $2029 \text{ cm}^{-1}$  band measured at 80 K for isothermal annealing at 180, 190, and 200 K are plotted in Fig. 6 versus the log of the annealing time. The dashed line in Fig. 6 illustrates the time dependence for an exponential decay rate of a first-order process. The observed decay in band intensity deviates sufficiently from an exponential so that the data cannot be appropriately analyzed to obtain an activation energy from a plot of unannealed fraction versus annealing time. However, when the initial conditions are the same for isothermally annealed samples, as they are in the present study, an activation energy can be determined by using a method of "cross cuts,"<sup>16</sup> independent of the order for the process, as discussed in Appendix A. In this method, the time to achieve a given unannealed fraction is obtained for different isothermal annealing temperatures. We use a closely related method,<sup>17</sup> which we call a method of

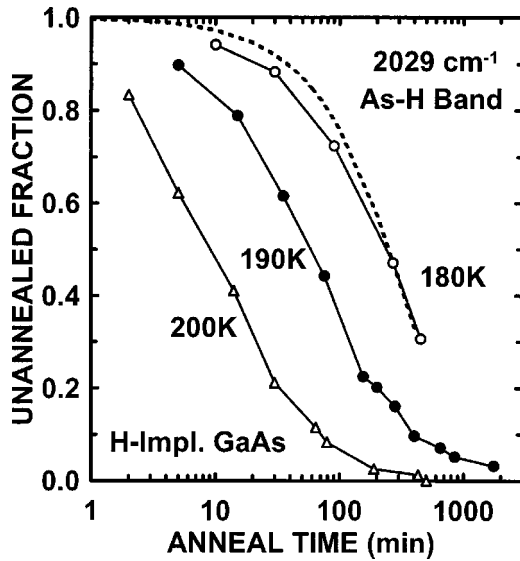


FIG. 6. Unannealed fraction of absorption by As-H centers versus annealing time at 180, 190, and 200 K after hydrogen implantation at 80 K. Dashed line illustrates a first-order decay rate.

“time ratios” wherein the time on one isothermal annealing curve is multiplied by an appropriate time ratio to superimpose this curve onto that for another annealing temperature. Figure 7 shows the As-H band decay curves superimposed on that for annealing at 180 K. The superposition was obtained by multiplying the annealing times at 190 and 200 K by “time ratios” of 5 and 28, respectively.

Figure 8 shows the increase in peak intensities for the Ga-H band with isothermal annealing time at 180, 190, and 200 K. Figure 9 shows the superposition of these growth curves using the same time ratios as those used for superpositioning the As-H decay curves. Although less satisfactory than the superposition for the As-H decay curves, the similarity between the temperature-time dependence for the loss of the As-H band and the growth of the Ga-H band is apparent. A relationship between As-H loss and Ga-H growth is further illustrated in Fig. 10 by plotting the As-H band intensity versus that for the Ga-H band through the annealing

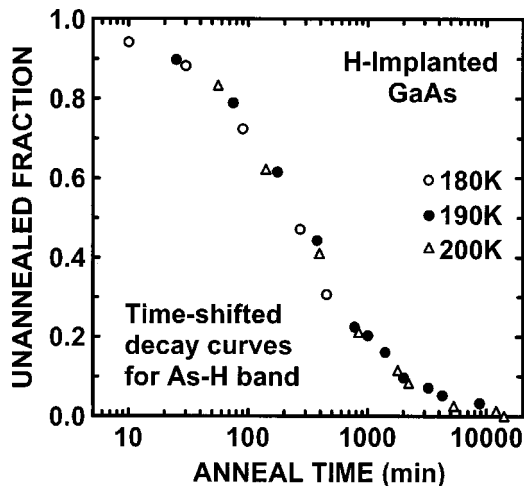


FIG. 7. Superposition of isothermal annealing curves of Fig. 6 obtained by multiplying the 190- and 200-K data points by “time ratios” of 5 and 28, respectively.

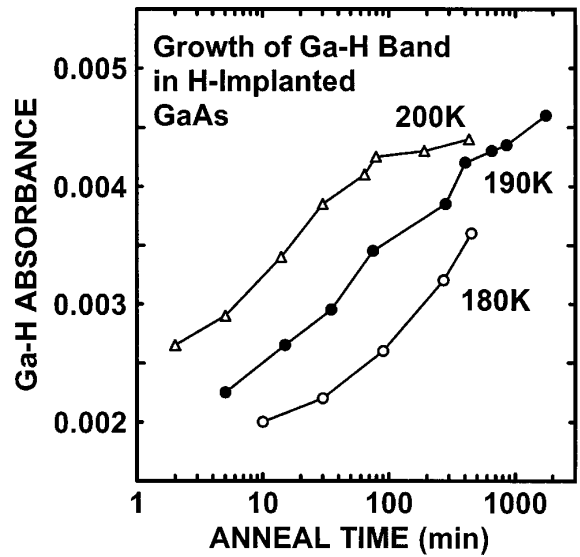


FIG. 8. Unannealed fraction of absorption for Ga-H centers versus annealing time at 180, 190, and 200 K after hydrogen implantation at 80 K.

steps. Note, however, that the loss rate for the peak intensity for the As-H band is a factor of 6 greater than that for the growth rate of the Ga-H band. In addition, the results presented in Fig. 2 show that the Ga-H band intensity continues to increase after the As-H band is no longer detectable. Thus, a hydrogen atom liberated from an As—H bond may jump several times or experience trap-limited mobility before re-trapping to form a Ga—H bond.

An Arrhenius plot of the time ratios from the isothermal annealing results for the As-H centers gives an activation energy of  $0.5 \pm 0.05$  eV as shown in Fig. 11. Since the same time ratios as those applied to the As-H centers give a reasonably good superposition for Ga-H center formation curves under isothermal annealing, the same activation energy is also assumed to apply for the growth of Ga-H centers.

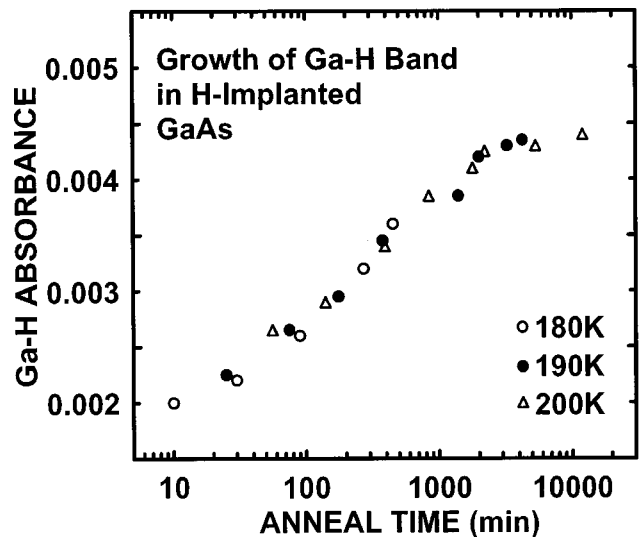


FIG. 9. Superposition of isothermal annealing curves of Fig. 8 obtained by multiplying the 190- and 200-K data points by time ratios of 5 and 28, respectively.

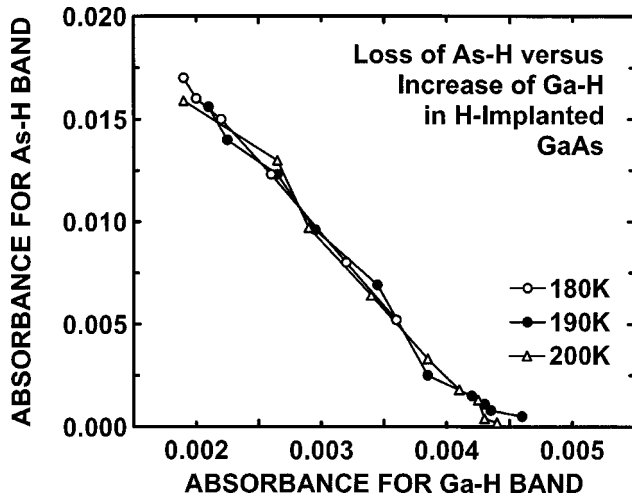


FIG. 10. Loss of absorption by As-H centers at 180, 190, and 200 K vs that for growth of Ga-H centers in GaAs after hydrogen implantation at 80 K.

#### IV. DISCUSSION

The experimental data clearly show chemical bonding of hydrogen to the As and Ga host constituents of GaAs following hydrogen implantation at 80 K. It is not clear, however, how to explain the partitioning of hydrogen between As—H and Ga—H bonds, or the thermal stability of the bonds. Atomic displacements by hard-sphere collisions in the implantation process are expected to occur nearly equally on the As and Ga sublattices<sup>14</sup> during implantations since there is little difference between the atomic mass of Ga and As. Bond energies for As—H and Ga—H are also nearly equivalent; bond dissociation energies for diatomic As—H and Ga—H molecules are 62 and 67 kcal/mole, respectively.<sup>18,19</sup> Furthermore, the observed predominance of As—H over Ga—H bonds is contrary to theoretical findings,<sup>20</sup> which predict that bond-centered hydrogen in GaAs will form a stronger bond with a lower electronegative Ga(3.28) neighbor than with the As(3.9) neighbor in an undamaged lattice. To seek an explanation for the observed results, therefore, we

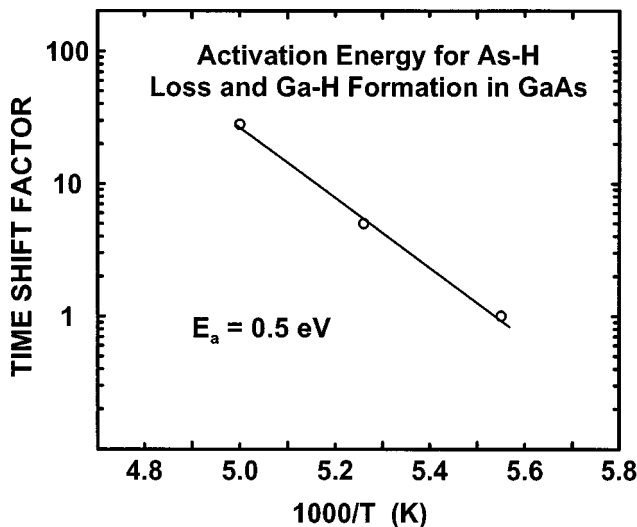


FIG. 11. Arrhenius plot of “time ratios” applied to superimpose isothermal annealing curves for As-H centers.

turn our attention to the nature and thermal stability of displacement defects produced by hydrogen implantation, hydrogen interaction with displacement defects, and the thermal stability of the defects.

It is known from other studies that hydrogen decorates displacement defects, and marks defects in annealing stages. In Si, for example, the annealing characteristics for an Si-H center produced by hydrogen implantation near 100 K were shown to correlate<sup>21</sup> with those for vacancies identified and characterized in EPR studies.<sup>22</sup> Previous studies on GaAs following hydrogen implantation at room temperature<sup>6–8</sup> have shown that annealing of Ga-H centers correlates with annealing of vacancy-interstitial pairs ( $V_{As}-As_i$ ) or  $V_{As}$  defects produced on the As sublattice. The As sublattice defect assignments were made in deep-level transient spectroscopy (DLTS) studies,<sup>23</sup> and the Ga-H centers observed in infrared absorption studies have been attributed to hydrogen bonded to Ga atom neighbors of displaced As atoms.<sup>8</sup>

We suggest that displacements on the Ga sublattice and multiple displacements in hydrogen implantation at 80 K create strain conditions and defects favorable for the formation of As-H centers. The release of hydrogen from bonds in these centers is attributed to annealing of defects that created the conditions favorable for formation of As—H bonds.

It is known that displacement defects produced in GaAs at low temperature introduce higher strain and a larger lattice expansion than the defects that remain, or are produced, at room temperature.<sup>9,12</sup> The defects that anneal below room temperature also exhibit a higher threshold energy for displacement than the defects that remain at room temperature.<sup>11,12</sup> Multiple displacements in a localized region have been suggested to explain the higher threshold energy and large lattice strain.<sup>11,12</sup>

Defects produced on the Ga sublattice are believed to play an important role in defect annealing below room temperature,<sup>11</sup> and Ga droplets have been reported near the surface of GaAs after exposure to a hydrogen plasma.<sup>24</sup> Thus, we have the possibility that interstitial Ga ( $Ga_i$ ) produced in GaAs at 80 K is mobile so that  $V_{Ga}-Ga_i$  pairs,  $Ga_i$ , and  $V_{Ga}$  are not stable at room temperature. An argument has been made that the Ga vacancy ( $V_{Ga}$ ) defects are generally not observed because they transform below room temperature into  $As_{Ga}As_3-V_{As}$  complexes.<sup>25</sup> Hydrogen, however, could possibly interact with  $V_{Ga}$  to produce a transformation to  $As_3As-H$  complexes yielding an As—H bond. Creighton<sup>18</sup> found As—H bonds are formed on weak or dangling bonds of GaAs surfaces under low dose atomic hydrogen exposure at 150 K. While formation rates are 4 to 5 times higher on an As-rich (100) surface, As—H bonds were formed on Ga-rich as well as on As-rich surfaces.<sup>18</sup> No explanation was put forth, but the results are suggestive of a chemical preference for As—H over Ga—H when GaAs is disordered by hydrogen ions at low temperature.

The absorption band characteristics for As-H centers we observe following hydrogen implantation at 80 K exhibit bandwidth characteristics that are similar to those reported previously<sup>8</sup> for the Ga-H absorption band produced by hydrogen implantation at room temperature. The bandwidths and measurement temperature dependence of the bandwidth and frequency, for both As-H and Ga-H centers, are large compared to those for hydrogen-related centers in as-grown

material.<sup>1</sup> Pajot and co-workers<sup>1</sup> noted that bandwidths for hydrogen-related complexes produced in compound semiconductors by hydrogen implantation can be two orders of magnitude larger than those in as-grown material, and the bandwidths increase further with increasing temperature. Thus, the bandwidth and temperature dependence of the bandwidth and frequency for the As-H band observed in the present study are consistent with bonding of hydrogen in a displacement-damaged host lattice.

Annealing stages below room temperature have been reported in a number of irradiation damage studies of GaAs. Annealing stages in GaAs centered near 235 and 280 K were observed in electrical measurements by Stein<sup>10</sup> and by Thommen<sup>11</sup> after electron irradiation of *n*-type GaAs at 80 K. An annealing stage at 235 K was also reported to occur after <sup>60</sup>Co  $\gamma$ -ray irradiation of *n*-type GaAs at 77 K.<sup>26</sup> Vook<sup>9</sup> reported lattice parameter and thermal conductivity measurements that showed defect annealing in GaAs below room temperature following electron irradiation. The thermal conductivity data showed two overlapping annealing stages centered near 225 and 300 K.<sup>9</sup> Recovery of thermal conductivity upon annealing is consistent with a removal of high lattice strain detected in measurements of the lattice parameter.

Pillukat and Ehrhart<sup>12</sup> suggested displacements on the Ga sublattice to explain the annealing stages below room temperature that they observed by changes in lattice parameter and associated large strain fields in high-dose electron irradiation of GaAs. According to the theoretical work of Estreicher,<sup>20</sup> hydrogen will be attracted to strained regions of a crystal where it can become trapped, often in a bound state. Correspondence of the annealing temperature for As-H centers with irradiation-produced defect annealing attributed to displacements on the Ga sublattice strengthens the suggestion that the implanted hydrogen initially decorates displacement defects created on the Ga sublattice.

The activation energy of  $0.5 \pm 0.05$  eV we determined for the loss of As-H centers by applying a method of time ratios (see Appendix A) is lower than the 0.72 eV reported by Thommen<sup>11(a)</sup> for the first-order annealing of electron irradiation damage in GaAs near 235 K. Further, the activation energy obtained here is similar to the range of binding energies (0.4–1.0 eV) for dopant H complexes suggested by Pearton.<sup>11(b)</sup> The annealing temperature for the loss of the As-H centers is also lower by  $\sim 50$  K than that for annealing of electron damage. Hydrogen trapping in a strain environment wherein hydrogen interacts chemically may allow a complex to relax toward a more favorable conformation and thus reduce the temperature and activation energy for annealing of the defects.

While temperatures of  $\approx 500$  K are necessary to release hydrogen from damage traps in implanted profiles after implantation at room temperature,<sup>27</sup> stress-alignment studies of Stavola *et al.*<sup>28</sup> on Be-H complexes in GaAs indicated that hydrogen moves among the four bond-centered configurations at 100 K with an activation energy of 0.37 eV. We infer from these results that hydrogen released from As bonds at temperatures  $\geq 110$  K will have sufficient mobility to reach additional trap sites such as Ga bonds within the buried damage layer to form Ga-H centers.

## V. SUMMARY AND CONCLUSIONS

An investigation of the LVM's produced by hydrogen implantation into GaAs at 80 K has been performed to examine hydrogen decoration of defects and their stability below room temperature. In contrast to the formation of Ga-H centers by hydrogen implantation at room temperature, As-H centers are formed by hydrogen implantation at 80 K. The apparent preferential formation of As—H bonds at 80 K is believed to involve lattice strain and selective bonding on defects produced on the Ga sublattice that expose weak and dangling As bond sites. A strong dependence of the frequency and bandwidth for the As-H absorption band on measurement temperature is in accord with disorder-related strain on the LVM of As—H bonds in GaAs. Annealing of the As-H absorption band after hydrogen implantation at 80 K occurs below room temperature, and in the same range of temperatures as those previously attributed to annealing of defects created on the Ga sublattice. An activation energy of  $0.5 \pm 0.05$  eV for annealing of the As-H centers following ion implantation was determined by an isothermal method. The activation energy is  $\approx 0.2$  eV lower than that associated with the annealing of Ga-related multiple displacement defects after electron irradiation. The reduction in activation energy for the hydrogen implanted layer is attributed to structural relaxation by the presence of As—H bonds within the multiple-displacement defects.

Absorption by Ga-H centers increases as absorption by As-H centers decreases upon annealing, and it continues to increase after As-H absorption is no longer detectable. We conclude that hydrogen is released from As—H bonds upon annealing of defects produced on the Ga sublattice, and it is retrapped on near-neighbor Ga atoms of the remaining As sublattice defects ( $V_{\text{As}}\text{-As}_i$  or  $V_{\text{Ga}}$ ) to produce the LVM for Ga-H. For hydrogen implantation of GaAs at room temperature, As-H centers and associated defects will be removed by annealing during implantation. Hence, only the LVM for Ga-H centers will be observed after implantations at room temperature.

## ACKNOWLEDGMENTS

The authors wish to thank Ken Minor for performing the hydrogen implantations. This work was performed at Sandia National Laboratories and supported by the U.S. Department of Energy Office of Basic Energy Sciences under Contract No. DE-AC04-94AL85000.

## APPENDIX A

The time rate of change for the defect concentration ( $dn/dt$ ) during isothermal annealing is described by the expression

$$dn/dt = K(T)f(n), \quad (\text{A1})$$

where  $K$  is a function of temperature  $T$ , but not of concentration  $n$  or time  $t$ .

Equation (A1) can be rewritten as  $dn/f(n) = K(T)dt$ , and for integration between the concentration limits  $n_0$  and  $n$ ,

$$\int_{n_0}^n dn/f(n) = K(T)t. \quad (\text{A2})$$

The left side of Eq. (A2) integrates to a constant  $C$  equal to the  $K(T)t$  product for a fixed value of  $n_0$  and any selected value for  $n$ . Assuming the temperature dependence for  $K(T)$  is given by the Boltzmann factor  $\exp(-E_a/kT)$ , where  $E_a$  is the activation energy for the annealing process and  $k$  is Boltzmann's constant,  $C = K' \exp(-E_a/kT)t$ . Rewriting Eq. (A2) as

$$C/t = K' \exp(-E_a/kT), \quad (\text{A3})$$

which illustrates the relationship between time and temperature for a selected  $n$  limit, as described by Eq. (A2) and assuming a single activation energy  $E_a$ . In the method of cross cuts,<sup>16</sup> annealing times to reach a selected  $n$  limit for two different annealing temperatures are used to evaluate  $E_a$ .

For a selected  $n$  limit, the ratio of annealing times,  $t_1$  and  $t_2$ , to reach the limit for two different isothermal annealing temperatures,  $T_1$  and  $T_2$ , is given by

$$t_2/t_1 = \exp(E_a/kT_1 - E_a/kT_2),$$

or

$$k \ln(t_2/t_1) = E_a(1/T_1 - 1/T_2), \quad (\text{A4})$$

where the constants  $C$  and  $K'$  cancel in the ratio. Selection of a different limit for  $n$  changes only the value of the constant  $C$ . Thus, Eq. (A4) applies for any selected value of  $n$  so that the difference in reciprocal temperatures is the same throughout two different annealing curves, and is related to the time ratio through  $E_a$ .

We used Eq. (A4) (the method of time ratios) to obtain an activation energy  $E_a$  from isothermal annealing data plotted as the unannealed fraction of As-H centers. For data plotted on a log time axis to display a wide range of decay time, multiplying the time by a time ratio factor produces a translation on the time axis to superposition decay curves from two different temperatures. The method of time ratios, therefore, utilizes all of the isothermal annealing data points obtained from the different isothermal temperatures to obtain a best fit for the shift in annealing time with annealing temperature.

It can be seen from an examination of Eq. (A4) that the slope obtained from an Arrhenius plot of  $k(\ln$  of the time ratios) against the reciprocal temperatures for different  $T_2$ , when holding  $T_1$  constant, will give a value for  $E_a$ .

- 
- <sup>1</sup>Jacques Chevallier, Bernard Clerjaud, and Bernard Pajot, in *Hydrogen in Semiconductors*, edited by J. I. Pankove and N. M. Johnson (Academic, New York, 1991), Chap. 13; Bernard Pajot, Bernard Clerjaud, and Jacques Chevallier, *Physica B* **170**, 371 (1991).
- <sup>2</sup>M. Stavola and S. J. Pearton, in *Hydrogen in Semiconductors* (Ref. 1), Chap. 8.
- <sup>3</sup>R. C. Newman, in *Semiconductors and Semimetals*, Vol. 36, edited by E. R. Weber (Academic, New York, 1993), Chap. 4.
- <sup>4</sup>J. A. Topich and R. A. Turi, *Appl. Phys. Lett.* **41**, 641 (1982).
- <sup>5</sup>G. D. Watkins, *Radiation Damage in Semiconductors* (Academic, New York, 1965), pp. 97–114.
- <sup>6</sup>R. C. Newman and J. Woodhead, *Radiat. Eff.* **53**, 41 (1980).
- <sup>7</sup>J. Tatarikiewicz, A. Krol, A. Breitschwerdt, and M. Cardona, *Phys. Status Solidi B* **140**, 369 (1987).
- <sup>8</sup>L. P. Wang, L. Z. Zhang, W. X. Zhu, X. T. Lu, and G. G. Qin, *Phys. Status Solidi B* **158**, 113 (1990).
- <sup>9</sup>F. L. Vook, *J. Phys. Soc. Jpn. Suppl. II* **18**, 190 (1963); *Phys. Rev.* **135**, A1742 (1964).
- <sup>10</sup>H. J. Stein, *J. Appl. Phys.* **40**, 5300 (1969).
- <sup>11</sup>(a) K. Thommen, *Radiat. Eff.* **2**, 201 (1970); (b) S. J. Pearton, *Mater. Sci. Forum* **148-149**, 393 (1994).
- <sup>12</sup>A. Pillukat and P. Ehrhart, *Mater. Sci. Forum* **83-87**, 947 (1992).
- <sup>13</sup>H. J. Stein and R. H. Baxter, *Rev. Sci. Instrum.* **45**, 1537 (1974).
- <sup>14</sup>J. F. Ziegler, J. P. Biersack, and U. Littmark, *The Stopping and Range of Ions in Solids* (Pergamon, New York, 1985); J. F. Ziegler (private communication).
- <sup>15</sup>H. J. Stein, *Appl. Phys. Lett.* **57**, 792 (1990); *Nucl. Instrum. Methods Phys. Res. B* **59/60**, 1106 (1991).
- <sup>16</sup>R. J. Borg and G. J. Dienes, *An Introduction to Solid State Diffusion* (Academic Press, San Diego, CA, 1988), Chap. X.
- <sup>17</sup>W. L. Brown, W. M. Augustyniak, and T. R. Waite, *J. Appl. Phys.* **30**, 1258 (1959).
- <sup>18</sup>J. R. Creighton, *J. Vac. Sci. Technol. A* **8**, 3984 (1990).
- <sup>19</sup>A. G. Gaydon, *Dissociation Energies and Spectra of Diatomic Molecules* (Chapman and Hall LTD, London, 1986), p. 270.
- <sup>20</sup>S. K. Estreicher, *Mater. Sci. Forum* **148-149**, 349 (1994).
- <sup>21</sup>H. J. Stein, *Phys. Rev. Lett.* **43**, 1030 (1979).
- <sup>22</sup>G. D. Watkins, *J. Phys. Soc. Jpn.* **18**, 22 (1963).
- <sup>23</sup>D. Pons, *Physica B & C* **116**, 388 (1983).
- <sup>24</sup>G. S. Jackson, J. Beberman, M. S. Feng, K. C. Hsieh, N. Holonyak, Jr., and J. Verdeyen, *J. Appl. Phys.* **64**, 5175 (1988).
- <sup>25</sup>H. J. von Bardeleben, J. C. Bourgoin, and A. Miret, *Phys. Rev. B* **34**, 1360 (1986).
- <sup>26</sup>E. Yu. Brailovskii and I. D. Konozenko, *Phys. Technics Semicond.* **5**, 641 (1971).
- <sup>27</sup>L. L. Liou, W. G. Spitzer, J. M. Zavada, and H. A. Jenkinson, *J. Appl. Phys.* **59**, 1936 (1986).
- <sup>28</sup>M. Stavola, S. J. Pearton, J. Lopata, C. R. Abernathy, and K. Bergman, *Phys. Rev. B* **39**, 8051 (1989).